Morphometric analysis of low mountains for mapping flash flood susceptibility in headwaters

Balázs Víg (vbalazs90@hotmail.com)
Pecsi Tudomanyegyetem Termeszettudomanyi Kar https://orcid.org/0000-0002-2506-396X
Szabolcs Ákos Fábián
Pecsi Tudomanyegyetem Termeszettudomanyi Kar
Szabolcs Czigány
Pecsi Tudomanyegyetem Termeszettudomanyi Kar
Ervin Pirkhoffer
Pecsi Tudomanyegyetem Termeszettudomanyi Kar
Ákos Halmai
Pecsi Tudomanyegyetem Termeszettudomanyi Kar
István Péter Kovács
Pecsi Tudomanyegyetem Termeszettudomanyi Kar
Gábor Varga
Pecsi Tudomanyegyetem Termeszettudomanyi Kar
József Dezső
Pecsi Tudomanyegyetem Termeszettudomanyi Kar
Gábor Nagy
Pecsi Tudomanyegyetem Termeszettudomanyi Kar
Dénes Lóczy
Pecsi Tudomanyegyetem Termeszettudomanyi Kar

Research Article

Keywords: morphometric indices, subwatershed prioritization, flash flood susceptibility, runoff, compactness, Mecsek Hills

Posted Date: March 11th, 2022

DOI: https://doi.org/10.21203/rs.3.rs-1318911/v1

Abstract

Morphometric indices from high-resolution DEMs can contribute to the estimation of flash flood susceptibility in mountainous areas. We have screened 25 morphometric indices commonly used in literature, and based on a correlation matrix, selected those which showed the strongest relationship with flash flood generation: area (*A*), drainage texture (*Rt*), drainage density (*Dd*), elongation ratio (*Re*), form factor (*Ff*), lemniscate method (*k)*, Gravelius coefficient (*GC)*, forested area (*Fa)* and relief ratio *(Rr)*. Among them *Dd, Rt* and *Rr* were in direct relationship with the probability of flash flood generation, while *A, Re, Fa, Ff, k* and *GC* are in inverse relationship with the intensity of flash floods. Our summary map shows the prioritization of the subwatersheds on a scale of 0 to 9. The flash flood risk ranking was empirically verified using 20-year water regime data obtained from 14 official stream gauges. Our conclusions only partially agree with former observations which may be explained by the particular lithology and morphology of the Mecsek Hills. Since the lower sections of the subwatersheds are urbanized, for optimal watershed management more detailed GIS analyses of anthropogenic controls on flash flood hazard are needed in the future.

1 Introduction

The shapes of watersheds may influence (flash) flood hazard (Gregory and Walling 1968). Therefore, the control of watershed morphology on local hydrology has been studied extensively and is a widely discussed scientific topic (Mangan et al. 2019). The earliest investigations aimed at determining the characteristics and regularities of the individual river basins using a large number of numerical indices (Strahler 1957). Mathematical formulae are often used to define the morphometry of catchments, stream networks and drainage patterns (Schumm 1956; Strahler 1957; Bogaert et al. 2000; Fryirs et al. 2007). Recent research has complemented the analyses through the use of GIS softwares, and in some cases has refined the existing and internationally approved procedures (Masoner and March 2006; Biswas 2016). However, it is also true that the reliability of GIS application depends on data quality, defined by the survey mode and the date of acquisition of the available databases (Lahsaini et al. 2018). Morphometric calculations based on high-resolution DEMs and other vector databases may provide a sound basis for runoff and flood susceptibility estimations.

Depending on the algorithm applied for watershed delineation, small headwater catchments and their watercourses account, by number, for about 60% of all drainage networks on Earth (Alexander et al. 2007). The analysis of their morphometric properties is crucial to understand the morphological evolution of river networks and the intensity of the hydrologic processes related to the water cycle operating on them, including both water retention and flooding (Bywater-Reyes et al. 2017).

Flash floods are a rather frequent phenomenon in the drainage basins of the hilly and low mountain regions of Hungary (Lóczy et al. 2012). Over the last decades, as a consequence of land use changes and global climate change, flash floods have been occurring with decreasing return periods and increasing severity (Pirkhoffer et al. 2009; Archer and Fowler 2021). One of the most flash flood-prone areas of Hungary is the Mecsek Mountains, with numerous reported flash flood events over the past decades (Gyenizse and Vass 1998). Although with reduced severity due to their low relative relief, the rolling hills of South Transdanubia (SW Hungary) are also frequently affected by flash floods (Czigány et al. 2008).

In addition to a wide range of factors, including climate, topography, land use types, soils and catchment morphometry, anthropogenic factors also control hydrological processes at catchment scale. The extent of the developed areas, percentage of sealed surfaces, infrastructural development, population density, and economic activity do not only have a landscape-modifying effect but also fundamentally influence the ratio of infiltration to runoff. Changes in land cover during commercial forestry operations and changes in the percentage of forested areas significantly control the amount of deadwood and woody debris accumulated in streambeds, hence hindering flow in the channel (Dixon and Sear 2014; Short et al. 2015; Galia et al. 2017, 2018).

Field research may provide an adequate basis for detailed river basin analyses (Kamykowska et al. 1999; Płaczkowska and Krzemień 2018). Surveys on both the morphological and land-use characteristics of catchments contribute to the understanding of the dynamics of watercourses and the general behaviour of the components of drainage systems (Fryirs et al. 2007a, b).

Hitherto, less attention has been paid to the study of the morphology of headwaters and their catchments both globally and in Hungary. Therefore, to authors' knowledge, a significant scientific gap exists in the field of headwater hydromorphometric studies. Hence, the present paper aims at morphometrically characterizing headwater catchments in the Mecsek Mountains in SW Hungary, which are representative for many low-mountain regions of Hungary and Central and Eastern Europe. Secondly, we intended to overview all available indices and to identify those which are most relevant for flash flood studies. A third objective was to contribute to the evaluation of flash flood hazard for headwater catchments in the Mecsek Mountains based on key morphometric parameters.

2 Study Area

The study area is located in the Mecsek Mountains (330 km^2) and the surrounding rolling terrain of South-Transdanubia, Hungary, where 53 drainage subbasins (654.5 km^2) were delineated based on a 10-meter resolution DEM. The elevation of the study area varies between 105 and 682 metres (a.s.l.) including both low-mountainous and hilly terrains. Relative relief averages between 120 and 240 m/km^2 and reaches maxima of 280–320 m/km^2, while it decreases to 40–80 m/km^2 in the foothill zone (Figs. 1 and 2).

Geologically the Mecsek is divided into two major structural units (Konrád and Sebe 2010); Haas 2013). The western unit has an anticline structure composed of Permian and Triassic sandstones, conglomerates and siltstones, while in the Central and Eastern Mecsek Jurassic and Cretaceous limestones, marls, shales and to a lesser degree dolomites prevail. Magmatic intrusions and interlayered volcanic materials (Mecsekjános Basalt Formation) are also found in the study area due to the tectonic movements in the Lower Cretaceous. The lower foothills and forelands covered by much younger lacustrine, fluvial and aeolian sediments from the Late Neogene and Quaternary periods.

As far as climate is concerned, the mean annual air temperature ranges from 7°C in the summit regions and increases to 12°C in wind-sheltered and south-facing slopes. Mean annual precipitation totals vary between 650 and 850 mm with some orographic surplus in the summit regions and decreasing annual totals to the south-eastern margin of the study area. Precipitation showed significant extremities in the last decades (e.g.

extreme highs in 2010 and 2014 and an extreme low in 2011) compared to the long-term averages (Hungarian Meteorological Service).

The watercourses of the Mecsek are drained by the Danube via four catchments. The River Karasica drains the Mecsek Mountains in its southern, south-eastern portion and conducts water directly to the Danube. The Pécsi-víz is the main recipient to the southwest, while the Baranya Canal, the River Kapos and the Sió system drain the waters to the north and northwest (Kocsis 2018).

Intensively managed deciduous forests cover about 320 km^2 within the studied catchments. The dominant species include European beech *(Fagus sylvatica)*, English oak (*Quercus robur*) and sessile oak *(Quercus petraea)* mixed variously with numerous other hardwood species. Only scattered stands of conifers are found in the area (Mecsek Forestry Co. Ltd.).

The soils of the studied area are highly diverse showing a rather heterogeneous distribution. Brown forest soils with significant clay accumulation in the B horizon (WRB: Luvisols, Soil Taxonomy: Alfisols-Hapludalfs) dominate the area, spotted with Leptic Umbrisols, Cambisols, Leptosols, Phaeozems, Rendzinas and Fluvisols (Soil Taxonomy: Entisols, Inceptisols and Histosols). Due to the intense anthropogenic interventions, their general conditions are often deteriorated (Kocsis 2018).

The study area has multiple communities and developed areas (as a legacy of uranium and coal mining), to which headwater hydrologic processes, including flash floods, may pose a significant threat. The largest city is Pécs with 140,237 residents as of 2021, while 61 other communities with a total population of 85,962 people are also found in the area. The main traffic route of national highway 6 and the main railway line connecting Pécs and the capital also passes through the area. The strategic protection of these transport routes from flooding and related mass movements is also of utmost importance.

3 Materials And Methods

Similarly to numerous studies (e.g., Tucker et al. 2001; Masoner and March, 2006; Czigány et al. 2008; Pareta and Pareta 2011), the watersheds were delineated from a hydrologically correct DEM of 10-meter resolution. ArcGIS 10.2 and the open-source ArcHydro Toolbox were used for morphometric analyses. The delineation of watershed boundaries was adjusted to the map of the national microregion classification presented in the National Atlas of Hungary (Kocsis 2018). In total, 53 watersheds have been delineated.

3.1 Calculation of areal parameters

In total, 25 hydromorphological parameters were calculated for each watershed, hence more than 1,500 numeric data were generated (Table 1). Among them 12 areal parameters were selected for analysis. Drainage pattern, topography and land use distribution were determined for each catchment. Beyond the fundamental geometric parameters (area and perimeter), ten commonly used morphometric indices were calculated, adapted for the physical characteristics of the study area (Schumm 1956, 1963; Strahler 1957; Morisawa 1962; Mesa 2006; Sassolas-Serrayet et al. 2018). Drainage density *(Dd)* is the ratio between the total length of the stream and the area of watershed and is commonly classified into 5 categories by former literature (Sukristiyanti et al. 2018 and Daipan 2020). The drainage texture ratio *(Rt)* is the total number of stream

segments of all order divided by the perimeter of the watershed (Horton 1945). Its division into classes is similar to that of drainage density. Maximum basin length (*L*) is determined as the diameter of the circle drawn around the margins of the catchment. Hack (1957) found correlation between catchment area and maximum basin length ($L=1.4 \bullet A^{0.6}$). Elongation ratio (*Re*) is the diameter of a circle of the same area as the basin over the maximum basin length (Sukristiyanti et al. 2018). The form factor (*Ff*) shows the ratio of basin area to the square of the maximum basin length (Mesa 2006; Daipan 2020; Sukristiyanti et al. 2018 referring to Horton 1945). Form factors above 0.78 indicate more circular watersheds while lower values (<0.78) refer to more elongated catchments. Circularity ratio (*Rc*) is the ratio of the watershed area to the area of a circle having the same circumference as the perimeter of the watershed (Daipan 2020). Moores (1966) defined the so-called lemniscate index *(k)* as a measure of deviation of the actual shape of the watersheds from the ideal shape. Chorley (1957) used a loop to measure the shape of drainage basins. If *k = 1*, the basin is circular and becomes more elongated with increasing *k* values (Moores 1966). The value of the Gravelius coefficient (*GC*) refers to the compactness of a watershed. GC is the ratio of the perimeter of the watershed to the circumference of a circle where area is equal to that of the given drainage basin (hence GC = 1 is a circle). The fitness ratio *(Rf)* (Pareta and Pareta 2011) or channel length to perimeter ratio (Melton 1957) is a dimensionless measure for the topographic pattern of watersheds.

Table 1 The formulae applied for watershed analysis. D = diameter of the circle of the same area as the basin

Parameters	Formula	References
Areal/geometry parameters		
Perimeter (P) [km]	–	–
Area (A) [km²]	–	–
Drainage texture (Rt)	$Rt = Nu/P$	(Horton 1945)
Max. basin length (L) [km]	–	(Kamykowska et al. 1999)
Integration index (C) [km²/km]	$C = A/L$	(Kamykowska et al. 1999)
Drainage density (Dd) [km/km²]	$Dd = \sum L/A$	(Strahler 1957)
Elongation ratio (Re)	$Re = D/L$	(Schumm 1956)
Form factor (Ff)	$Ff = A/L^2$	(Mesa 2006)
Circularity ratio (Rc)	$Rc = 4\pi A/P^2$	(Mesa 2006)
Lemniscate index (k)	$k = L^2\pi/4A$	(Moores 1966)
Gravelius coefficient (GC)	$GC = P/2\sqrt{\pi A}$	(Sassolas-Serrayet et al. 2018)
Fitness ratio (Rf)	$Rf = Cl/P$	(Pareta and Pareta 2011)
Linear parameters		
Number of streams (Nu)	–	–
Stream length (SL) [km]	–	–
Total stream length (ΣL) [km]	–	–
Max stream order (u max)	–	(Morisawa 1962)
Total length of stream orders (Σu) [km]	–	–
Mean stream length (Lu) [km]	$Lu = SL/Nu$	(Biswas 2016)
Length of main channel (Cl) [km]	–	–
Relief parameters		
Maximum height (H); minimum height (h) [m]	–	–
Basin relief (r) [m]	$r = H - h$	–
Relief ratio (Rr)	$Rr = H - h/L$	(Schumm 1956)
Land use parameters		
Forested area (Fa) [%]	–	(Kamykowska et al. 1999)
Grassland area (Ga) [%]	–	(Kamykowska et al. 1999)
Arable land area (Aa) [%]	–	(Kamykowska et al. 1999)

3.2 Calculation of linear parameters

The vector-based GIS database of the channel network of Hungary, provided by the South Transdanubian Water Directorate (DDVÍZIG, Pécs), was used for the calculation of linear parameters. Seven linear parameters were calculated for each watershed (Table 1) using the approaches by Apaydin et al. (2006) and Biswas (2016).

3.3 Calculation of topographic and land use parameters

The topographic parameters considered were relative relief and relief ratio. The latter is calculated as the difference of the highest and lowest point of the catchment divided by maximum basin length (*L*). According to Daipan (2020) and Schumm (1956) relief ratio *(Rr)* is a ratio between the total relief of the watershed (difference the highest and lowest elevation in m) and the maximum catchment length. The Corine Land Cover 2012 database was used to spatially analyse the distribution of land use types of the area (Kamykowska et al. 1999). Statistical calculations were performed in Microsoft Excel software environment.

Based on the analysis of morphometric parameters watershed prioritization (Kadam et al. 2016; Abdo 2020) was employed for establishing flash flood susceptibility. Susceptibility levels were ranked on a linear scale of 0 to 9 (0 = lowest, 9 = highest). Susceptibility was prioritized and mapped for each subwatershed using averaged ranks.

3.4 Hydrological verification

The time series of stream gauge data from 14 sites (a-n) obtained from the Directorate DDVÍZIG were applied for verification (see Fig. 1). Although these time series vary in length (4-21 years), we believe that the number of flash flood events is relevant for our topic. Flash floods were defined as marked maxima of water discharge for the individual gauges. Consequently, the events in the last three and last two bins on histograms prepared from the water discharge fluctuations of two dates of measurement (typically 15 minutes to 60 minutes) were investigated. Since the properties of time series for each gauge are individual (regarding minima, maxima and mean values), the province between minimum and maximum were divided into ten equal bins in all cases.

4 Results And Discussion

Our formulae were grouped based on areal/geometric properties, linearity, relief and land use presented in former literature (Srinivasa Vittala et al. 2004; Farhan et al. 2016; Fenta et al. 2017; Daipan 2020). Although we aimed at adjusting our analyses to the formerly published systems, some minimal subjectivity was unavoidable during the classifications. Table 2 shows the investigated morphometric parameters employed in the current study.

Table 2 The fundamental descriptive statistics for all calculated parameters with the exception of land use (Fa, Ga, Aa **).**

	n	Mean	Median	Std.Dev.	Kurtosis	Skewness	Min	Max
Areal/geometry parameters								
P	53	24.10	24.46	7.00	3.28	0.72	8.56	51.36
A	53	12.35	12.49	6.62	3.66	1.43	1.45	37.30
Rt	53	0.22	0.18	0.18	3.32	1.65	0.03	0.84
L	53	7.04	7.00	2.32	5.82	1.45	2.60	17.11
C	53	1.70	1.67	0.58	0.23	0.65	0.56	3.25
Dd	53	0.90	0.91	0.33	-0.42	-0.25	0.16	1.57
Re	53	0.56	0.55	0.10	0.18	0.32	0.32	0.82
Ff	53	0.26	0.24	0.09	0.64	0.83	0.08	0.53
Rc	53	0.26	0.26	0.06	0.28	0.34	0.11	0.43
k	53	3.52	3.25	1.45	5.2	1.79	1.47	9.59
GC	53	2.00	1.97	0.26	2.33	1.00	1.53	2.97
Rf	53	0.25	0.02	0.12	5.42	1.02	0.00	0.77
Linear parameters								
Nu	53	5.62	4.00	5.00	3.53	1.78	1.00	23.00
ΣL	53	11.13	9.78	7.19	1.81	1.18	1.05	36.27
u max	53	2.30	2.00	0.85	-0.51	1.16	1.00	4.00
Lu	53	2.59	2.15	1.63	9.73	2.70	1.05	10.43
Cl	53	6.2	6.39	2.9	-0.5	0.15	1.05	13.15
Relief parameters								
H	53	473.83	488.62	130.33	-1.06	-0.31	200.58	679.92
h	53	154.20	151.54	33.91	-0.24	0.63	105.13	224.29
r	53	319.63	332.38	123.47	-1.15	-0.20	93.70	541.90
Rr	53	48.39	46.0	20.53	-0.15	0.39	9.46	96.9

4.1 Areal and geometric parameters

At this level of detail areas of the studied watersheds ranged from 1.45 to 37.3 km^2. According to the classification scheme proposed by Daipan (2020) they belong to the micro ($A \leq 10$ km^2, n = 20) and small (A = 10 to 100 km^2, n = 33) watershed categories. In accordance with the findings of Zavoianu (1985), performed on watersheds of hilly and mountainous terrains, we found a close linear correlation between catchment perimeters and catchment area with an R^2 = 0.78 (Fig. 8). The general inverse relationship between watershed

size and flash flood susceptibility, therefore, suggests high levels of flash flood hazard for the study area (Daipan 2020).

This is explained by the rapid hydrologic response due to the steepness of slopes of small headwater catchments and the surplus precipitation of orographic origin. In terms of runoff intensity, the short times of concentration have already been documented for the small headwater catchments of the Mecsek Mountains (Czigány et al. 2008).

For drainage texture (*Rt*) all studied watershed belong to the very coarse class (low drainage density) as its value was found to be less than 2 km km^{-1} in all cases. The low surface density of drainage is likely explained by the jointing of limestone and the relatively dense vegetation cover in the majority of the area (mean forest cover: 46.5%). These properties reduce flash flood susceptibility.

Maximum catchment lengths (*L*) varied broadly, spanning between 2.60 and 17.11 km. Maximum basin length, in accordance with our presumptions, showed a close relationship with watershed areas and perimeters *(R^2 =* 0.62 and 0.85, respectively) (Fig. 8). The *L* value is assumed to be inversely proportional with flash flood susceptibility.

Drainage density (*Dd*) is supposed to be closely correlated with lithology and the tectonic evolution of the catchment (Tucker et al. 2001). Others found correlation between relative relief and *Dd* value (Nag 1998). Our results revealed no correlation with basin relief (R^2 = 0.003) (Fig. 8). Calculated *Dd* varied between 0.16 and 1.57 with a standard deviation of 0.33. Based on the available classification of the aforementioned two literary sources, the studied watersheds belong to the group of very low drainage density catchments (*Dd* < 2 km km^{-1}). Adopting the results of Melton (1957) to our study site, we found different *Dd* values for watersheds of different area and identical lengths. Low *Dd* values indicate basins of relatively low surface stream density and a prolonged hydrologic response and refer to permeable near-surface rocks, dense vegetation and low relief (Sukristiyanti et al. 2018).

Computed low elongation ratios ($\bar{x}$ = 0.56) demonstrate that the majority of the analysed watersheds are elongated (0.5–0.7, n = 33) or highly elongated (< 0.5, n = 13). Only a minority of them are less elongated (0.7–0.8, n = 6) and oval (0.8–0.9, n = 1). The large number of elongated and highly elongated basins suggests younger and neotectonic evolution, whereas oval and circular basins show higher runoff intensity. This finding corroborates the results of Daipan (2020); Elsadek et al. (2019) and Sukristiyanti et al. (2018). Furthermore, the low *Re* values indicate low flood hazard in basins 5, 48, 51 and 53 (*Re* = 0.44, 0.32, 0.37 and 0.47, respectively). In contrast, the high *Re* values of basins 12, 19, 21 and 35 (0.71, 0.76, 0.75 and 0.82, respectively) likely demonstrate intense erosion and high flash flood hazard. Elongated watersheds are usually characterized by longer distances between the adjacent confluences (hydrographic nodes), low peak flows and broader hydrographs. All studied watersheds have low form factors. Therefore, are considered to be elongated rather than circular (0.08–0.53). This parameter did not provide any additional information on flood hazard.

Circularity ratio (Rc), essentially the same as elongation ratio and form factor, of less than 0.5 were found for all studied watersheds of the current study, again indicating low runoff. The calculated lemniscate (*k*) values (1.47 to 9.59) in our study are dominantly high, hence, similarly to the circularity ratio, indicate elongated catchments. This finding also confirms the fact that reduced *k* values are coupled with increasing stream

orders. Gravelius coefficients (GC) of 1.53 to 2.97 were found for the watersheds from which GC values of 1.7 to 2.1 covered 68% of the total area. According to the classification of Sassolas-Serrayet et al. (2018), 25 catchments (47.1%) with a total area of 295.7 km^2 (45.4% of the mountainous area) belong to the group of elongated (GC ≥ 2) catchments.

In correspondence to previous literature, maximum basin length showed a markedly higher correlation with catchment area (R^2 = 0.67) than with stream length (Fig. 8). It was due to the inaccuracy of the drainage network database, where streams with order = 1 were not included (Fig. 3).

4.2 Linear parameters

For the stream order we used the traditional hierarchical ranking by Strahler (1957). The lowest and the highest orders and the number of stream segments in the studied basins are shown in Table 2. The maximum Strahler orders (u_{max}) in the studied catchments were found to be dominantly between 1 and 3. Watercourses of Strahler order of 3 (n = 4) were only found in the periphery of the studied area (Figs. 4 and 5 and 6). Total stream lengths (ΣL) varied between 1.05 and 36.27 km. We found a correlation of R^2 = 0.75 between the two parameters which points out that number of streams is associated with greater total length (Fig. 8).

4.3 Topographic parameters

Properties associated with relief were characterized by the parameters of maximum height (*H*), minimum height (*h*), basin relief (*r*) and relief ratio (*Rr*). The highest (*H*) and the lowest (*h*) points of the studied catchments are located at elevations of 201 to 680 m and 105 to 224 m, respectively (Fig. 6). Basin relief changes in close correlation with *H* (R^2 = 0.93) (Fig. 8). In accordance with former findings (Daipan 2020), relief ratio was also found higher for watersheds of smaller area.

4.4 Land use parameters

In accordance with the findings of Kamykowska et al. (1999), we revealed that response times of flash floods in the studied area are significantly controlled by land use, i.e. the extent of forests (Fa), grasslands (Ga) and arable land (Aa). Percentage forest cover in the headwaters was found especially influential on delaying and mitigating runoff and changing the proportions of evaporation, infiltration, and surface runoff. Percentage of forests, strongly correlated with high relief and higher elevation, exceeds 70% in the studied subwatersheds. (The average ratio of forests is 23.4% for the Mecsek Hills.) However, the higher percentage of forested areas contributes to an intense production of woody debris contributing to flash flooding in the area through hindering runoff. In the foothill areas of lower elevation arable lands dominate the subwatersheds, while the total area of natural pastures is negligible (Fig. 7).

4.5 Flash flood susceptibility

Among the topographical factors discussed by former literature (Esper Angillieri 2008; Singh et al. 2013; Abdel-Fattah et al. 2017; Puno and Puno 2019; Alam et al. 2020; Obeidat et al. 2020) the following parameters have been selected for analysis: area *(A)*, drainage texture *(Rt)*, drainage density *(Dd)*, elongation ratio *(Re)*, form factor *(Ff)*, lemniscate index *(k)*, Gravelius coefficient *(GC)*, forested area *(Fa)*, relief ratio *(Rr)*. Among them *A, Dd* and *Rr* were in direct relationship with the probability of flash flood generation, while *Rt, Re, Fa, Ff, k* and *GC*

are in inverse relationship with flash floods. All selected factors are related to runoff intensity and flash flood generation; hence they are applicable for the evaluation of flood susceptibility at watershed levels.

On the flood susceptibility map based on morphometric parameters subwatersheds were ranked on a linear scale of 0 to 9 (0 = lowest, 9 = highest) (Fig. 9). We revealed that the parameters most significantly contributed to flash flood generation were subwatershed size (small or medium) and compactness. Runoff was further intensified by high relief and low forest cover. The subwatersheds of the highest flood susceptibility (7 to 9) were 2, 10, 12, 16, 19, 29, 35, 49, while the lowest susceptibility (0 to 4) was found for watersheds of large area, elongated shape, low relief and extensive forest cover (5, 13, 15, 17, 18, 31, 32, 38).

Our results partly corroborated the findings of previous modelling which had been based on the spatial distribution of precipitation totals and intensities (e.g., Lóczy et al. 2012b). The spatial distribution of flash flood susceptibility showed a good spatial correspondence with the documented locations of flash flood events in the Mecsek Mountains (subwatersheds 2, 7, 12, 19, 16, 41, 46, 47, 49) (Pirkhoffer et al. 2009).

In contrast, ranking purely based on morphometric parameters performed somewhat poorly in the south-central part of the studied area (downtown Pécs, subwatersheds 36, 39, 40, 45, 48). Here, urban development, improper maintenance of hydrologic structures used for flood mitigation and smooth conveyance of stormwater and large extent of impervious surfaces may significantly increase runoff and may alter flow directions. Such factors increase the actual flood potential of these subwatersheds (Czigány et al. 2010).

From the comparison of watershed ranking for flash flood susceptibility with discharge data of official stream gauges, the following conclusions have been drawn. The number of events undoubtedly qualified as flash floods and the susceptibility rank established from shape, morphological, relief and land use variables do not correlate (R^2=0.28) (Fig. 10).

It should be noted that this statistical result is essentially distorted by a range of factors. Out of the 53 studied water discharge data are available in ten cases and they are asymmetrically distributed. Furthermore, there are four additional subwatersheds with two gauges. The outlets of the delineated subwatershed do not coincide with the gauges and the available date series do not cover the same period.

5 Conclusions

We used 25 morphometric parameters to characterize the 53 subwatersheds of the Mecsek Mountains. Based on the computed parameters, the subwatersheds were evaluated and prioritized according to their flash flood susceptibility.

The western part of the range is the northern wing of an anticline and the steep southern slopes are part of a tectonic window. The morphometry of the western Mecsek reflects high levels of ruggedness, variable lithology (sandstone) and intense tectonics all of which indirectly contribute to flash flood generation. According to the final ranking map (Fig. 9) the watersheds of the core area of the western Mecsek have high flash flood susceptibility.

Nonetheless, the high flash flood susceptibility should not be exclusively attributed to specific morphometric traits. Flash flood events are rather triggered by extreme runoffs due to intense meteorological events, further

augmented by inappropriate landscape management and altered land use patterns due to human interventions. Our findings refer to the headwater sections of low-mountains in the humid and semi-humid temperate zone, where the mosaic pattern of partially urbanized areas and forested lands dominate the landscape.

For the more profound investigation of urban catchments, an analysis of micro watersheds DEMs of submeter resolution and GIS databases of urban drainage utility networks would be indispensable (Burns et al. 2015; Towsif Khan et al. 2020). Such improvements are expected to increase the efficiency of flash flood prediction in urban areas and may decrease flood-related loss of lives and economic damage.

Declarations

Funding

This research was funded by the Higher Education Institutional Excellence Program of Ministry of Human Capacities (Hungary), grant number “20765-3/2018/FEKUTSTRAT” at the University of Pécs and the Hungarian National Office for Research and Innovation (project GINOP-2.3.2-15-2016-00055).

Competing Interests

The authors have no relevant financial or non-financial interests to disclose.

Author Contributions

All authors contributed to the study conception and design. Preparation and implementing of field-work were performed by Balázs Víg, Gábor Varga and Szabolcs Ákos Fábián. Data collection from national services were performed by Gábor Nagy and József Dezső. GIS analysis were performed by Balázs Víg, István Péter Kovács, Ákos Halmai and Ervin Pirkhoffer. The first draft of the manuscript was written by Balázs Víg, Szabolcs Ákos Fábián, Szabolcs Czigány and Dénes Lóczy and all authors commented on previous versions of the manuscript. All authors read and approved the final manuscript.

References

1. Abdo HG (2020) Evolving a total-evaluation map of flash flood hazard for hydro-prioritization based on geohydromorphometric parameters and GIS–RS manner in Al-Hussain river basin, Tartous, Syria. Nat Hazards 104:681–703. https://doi.org/10.1007/s11069-020-04186-3
2. Alam A, Ahmed B, Sammonds P (2020) Flash flood susceptibility assessment using the parameters of drainage basin morphometry in SE Bangladesh. Quat Int. https://doi.org/10.1016/j.quaint.2020.04.047
3. Alexander RB, Boyer EW, Smith RA, et al (2007) The role of headwater streams in downstream water quality. JAWRA J Am Water Resour Assoc 43:41–59. https://doi.org/10.1111/j.1752-1688.2007.00005.x
4. Apaydin H, Ozturk F, Merdun H, Aziz NM (2006) Determination of the drainage basin characteristics using vector GIS. Hydrol Res 37:129–142. https://doi.org/10.2166/nh.2006.0011
5. Biswas SS (2016) Analysis of GIS based morphometric parameters and hydrological changes in Parbati River basin, Himachal Pradesh, India. J Geogr Nat Disasters 6: 175. https://doi.org/10.4172/2167-

0587.1000175

6. Bogaert J, Rousseau R, Van Hecke P, Impens I (2000) Alternative area-perimeter ratios for measurement of 2D shape compactness of habitats. Appl Math Comput 111:71–85. https://doi.org/10.1016/S0096-3003(99)00075-2
7. Burns MJ, Schubert JE, Fletcher TD, Sanders BF (2015) Testing the impact of at-source stormwater management on urban flooding through a coupling of network and overland flow models. WIREs Water 2:291–300. https://doi.org/10.1002/wat2.1078
8. Bywater-Reyes S, Segura C, Bladon KD (2017) Geology and geomorphology control suspended sediment yield and modulate increases following timber harvest in temperate headwater streams. J Hydrol 548:754–769. https://doi.org/10.1016/j.jhydrol.2017.03.048
9. Chorley RJ (1957) Illustrating the laws of morphometry. Geol Mag 94:140–150. https://doi.org/10.1017/S0016756800068412
10. Czigány S, Pirkhoffer E, Balassa B, et al (2010) Villámárvíz mint természeti veszélyforrás a Dél-Dunántúlon (Flash floods as natural hazards in Southern Transdanubia). Földrajzi Közlemények 134:281–298
11. Czigány S, Pirkhoffer E, Geresdi I (2008) Environmental impacts of flash floods in Hungary. In: Samuels P, Huntington S, Allsop W, Harrop J (eds) Flood risk management: research and practice. CRC Press, pp 1439–1447
12. Daipan BPO (2020) Geomorphometric characterization and analysis of the Bued watershed using advanced spaceborne thermal emission and reflection radiometer – global digital elevation model V3 through geospatial techniques. Philipp J Sci 149:955–967
13. Dixon SJ, Sear DA (2014) The influence of geomorphology on large wood dynamics in a low gradient headwater stream. Water Resour Res 50:9194–9210. https://doi.org/10.1002/2014WR015947
14. Elsadek WM, Ibrahim MG, Mahmod WE, Kanae S (2019) Developing an overall assessment map for flood hazard on large area watershed using multi-method approach: case study of Wadi Qena watershed, Egypt. Nat Hazards 95:739–767. https://doi.org/10.1007/s11069-018-3517-3
15. Esper Angillieri MY (2008) Morphometric analysis of Colangüil river basin and flash flood hazard, San Juan, Argentina. Environ Geol 55:107–111. https://doi.org/10.1007/s00254-007-0969-2
16. Farhan Y, Elmaji I, Khalil O (2016) GIS-based morphometric analysis of fourth-order sub-basins of the Zerqa river (Northern Jordan) using multivariate statistical techniques. Nat Resour 07:461–480. https://doi.org/10.4236/nr.2016.78048
17. Fenta AA, Yasuda H, Shimizu K, et al (2017) Quantitative analysis and implications of drainage morphometry of the Agula watershed in the semi-arid northern Ethiopia. Appl Water Sci 7:3825–3840. https://doi.org/10.1007/s13201-017-0534-4
18. Fryirs KA, Brierley GJ, Preston NJ, Kasai M (2007a) Buffers, barriers and blankets: The (dis)connectivity of catchment-scale sediment cascades. Catena 70:49–67. https://doi.org/10.1016/j.catena.2006.07.007
19. Fryirs KA, Brierley GJ, Preston NJ, Spencer J (2007b) Catchment-scale (dis)connectivity in sediment flux in the upper Hunter catchment, New South Wales, Australia. Geomorphology 84:297–316. https://doi.org/10.1016/j.geomorph.2006.01.044
20. Galia T, Ruiz-Villanueva V, Tichavský R, et al (2018) Characteristics and abundance of large and small instream wood in a Carpathian mixed-forest headwater basin. For Ecol Manage 424:468–482.

https://doi.org/10.1016/j.foreco.2018.05.031

21. Galia T, Šilhán K, Ruiz-Villanueva V, et al (2017) Temporal dynamics of instream wood in headwater streams draining mixed Carpathian forests. Geomorphology 292:35–46. https://doi.org/10.1016/j.geomorph.2017.04.041
22. Gregory KJ, Walling DE (1968) The variation of drainage density within a catchment. Int Assoc Sci Hydrol Bull 13:61–68. https://doi.org/10.1080/02626666809493583
23. Gyenizse P, Vass P (1998) A természeti környezet szerepe a Nyugat-Mecsek településeinek kialakulásában és fejlödésében (The role of the physical environment in the development of settlement in the Western Mecsek Mountains). Foldr Ert 47:131–148
24. Horton RE (1945) Erosional development of streams and their draniage basins; hydrophysical approach to quantiative morphology. Geol Soc Am Bull 56:275
25. Kadam A, Umrikar B, Sankhua RN (2016) Geomorphometric characterization and priorization of watershed from semi-arid region, India for green growth potential. J Environ Reasearch Dev 11:417–432
26. Kamykowska M, Kaszowski L, Krzemien K (1999) River channel mapping instruction. Key to the river bed descreption. In: Krzemien K (ed) River channels. Pattern, structure and dynamics. Institute of Geography of the Jagiellonian University, Krakow, pp 9–25
27. Kocsis K (ed) (2018) National Atlas of Hungary. MTA CSFK Geographical Institute, Budapest
28. Konrád G, Sebe K (2010) Fiatal tektonikai jelenségek új észlelései a Nyugati-Mecsekben és környezetében (New details of young tectonic phenomena in the Western Mecsek Mts and their surroundings). Földtani Közlöny 140:135–162
29. Krzemien K (1999) River channels-pattern, structure and dynamics. Institute of Geography of the Jagiellonian University, Krakow
30. Lahsaini M, Tabyaoui H, Mounadel A, et al (2018) Comparison of SRTM and ASTER derived digital elevation models of Inaouene river watershed (North, Morocco) – Arc Hydro Modeling. J Geosci Environ Prot 06:141–156. https://doi.org/10.4236/gep.2018.69011
31. Loczy D, Czigany S, Pirkhoffer E (2012) Flash flood hazards. In: Kumarasamy M (ed) Studies on Water Management Issues. InTech, pp 27–52
32. Mangan P, Haq MA, Baral P (2019) Morphometric analysis of watershed using remote sensing and GIS – a case study of Nanganji River Basin in Tamil Nadu, India. Arab J Geosci 12:202. https://doi.org/10.1007/s12517-019-4382-4
33. Masoner JR, March F (2006) Geographic information systems methods for determining drainage-basin areas, stream-buffered areas, stream length, and land uses for the Neosho and Spring rivers in Northeastern Oklahoma. Scientific investigations report 2006-5293, USGS
34. Melton MA (1957) An analysis of the relations among elements of climate, surface properties, and geomorpholgy. Department of Geology, Columbia University, Technical report (United States, Office of Naval Research), no. 11
35. Mesa LM (2006) Morphometric analysis of a subtropical Andean basin (Tucumán, Argentina). Environ Geol 50:1235–1242. https://doi.org/10.1007/s00254-006-0297-y
36. Moores EA (1966) Regional drainage basin morphometry. Iowa State University, Digital Repository

37. Morisawa ME (1962) Quantitative geomorphology of some watersheds in the Appalachian plateau. GSA Bull 73:1025–1046. https://doi.org/10.1130/0016-7606(1962)73[1025:QGOSWI]2.0.CO;2
38. Pareta K, Pareta U (2011) Quantitative morphometric analysis of a watershed of Yamuna basin, India using ASTER (DEM). Data and Gis. Int J Geomatics Geosci 2:248–269
39. Pirkhoffer E, Czigány S, Geresdi I (2009) Impact of rainfall pattern on the occurrence of flash floods in Hungary. Zeitschrift für Geomorphol Suppl Issues 53:139–157. https://doi.org/10.1127/0372-8854/2009/0053S3-0139
40. Płaczkowska E, Krzemień K (2018) Natural conditions of coarse bedload transport in headwater catchments (Western Tatras, Poland). Geogr Ann Ser A, Phys Geogr 100:370–387. https://doi.org/10.1080/04353676.2018.1522957
41. Sassolas-Serrayet T, Cattin R, Ferry M (2018) The shape of watersheds. Nat Commun 9:3791. https://doi.org/10.1038/s41467-018-06210-4
42. Schumm SA (1956) Evolution of drainage systems and slopes in badlands at Perth Amboy, New Jersey. Bull Geol Soc Am 67:597–646
43. Schumm SA (1963) Sinuosity of alluvial rivers on the great plains. GSA Bull 74:1089–1100
44. Short LE, Gabet EJ, Hoffman DF (2015) The role of large woody debris in modulating the dispersal of a post-fire sediment pulse. Geomorphology 246:351–358. https://doi.org/10.1016/j.geomorph.2015.06.031
45. Singh P, Thakur JK, Singh UC (2013) Morphometric analysis of Morar River Basin, Madhya Pradesh, India, using remote sensing and GIS techniques. Environ Earth Sci 68:1967–1977. https://doi.org/10.1007/s12665-012-1884-8
46. Srinivasa Vittala S, Govindaiah S, Honne Gowda H (2004) Morphometric analysis of sub-watersheds in the pavagada area of Tumkur district, South India using remote sensing and gis techniques. J Indian Soc Remote Sens 32:351–362. https://doi.org/10.1007/BF03030860
47. Strahler AN (1957) Quantitative analysis of watershed geomorphology. Trans Am Geophys Union 38:913. https://doi.org/10.1029/TR038i006p00913
48. Sukristiyanti S, Maria R, Lestiana H (2018) Watershed-based morphometric analysis: a review. IOP Conf Ser Earth Environ Sci 118:012028. https://doi.org/10.1088/1755-1315/118/1/012028
49. Towsif Khan S, Chapa F, Hack J (2020) Highly resolved rainfall-runoff simulation of retrofitted green stormwater infrastructure at the micro-watershed scale. Land 9:339. https://doi.org/10.3390/land9090339
50. Tucker GE, Catani F, Rinaldo A, Bras RL (2001) Statistical analysis of drainage density from digital terrain data. Geomorphology 36:187–202. https://doi.org/10.1016/S0169-555X(00)00056-8
51. Zavoianu I (1985) Morphometry of drainage basins. Elsevier
52. Hungarian Meteorological Service (accessed October 10 2021) Climate of Hungary – general characteristics. https://www.met.hu/en/eghajlat/magyarorszag_eghajlata/altalanos_eghajlati_jellemzes/altalanos_leiras/

Figures

Figure 1

Elevation and stream network of the study area. 1: border of Mecsek micro landscape unit, 2: stream network.

Figure 2

Various types of the watershed according to Gravelius coefficient and its histogram. According to (Sassolas-Serrayet et al. 2018).

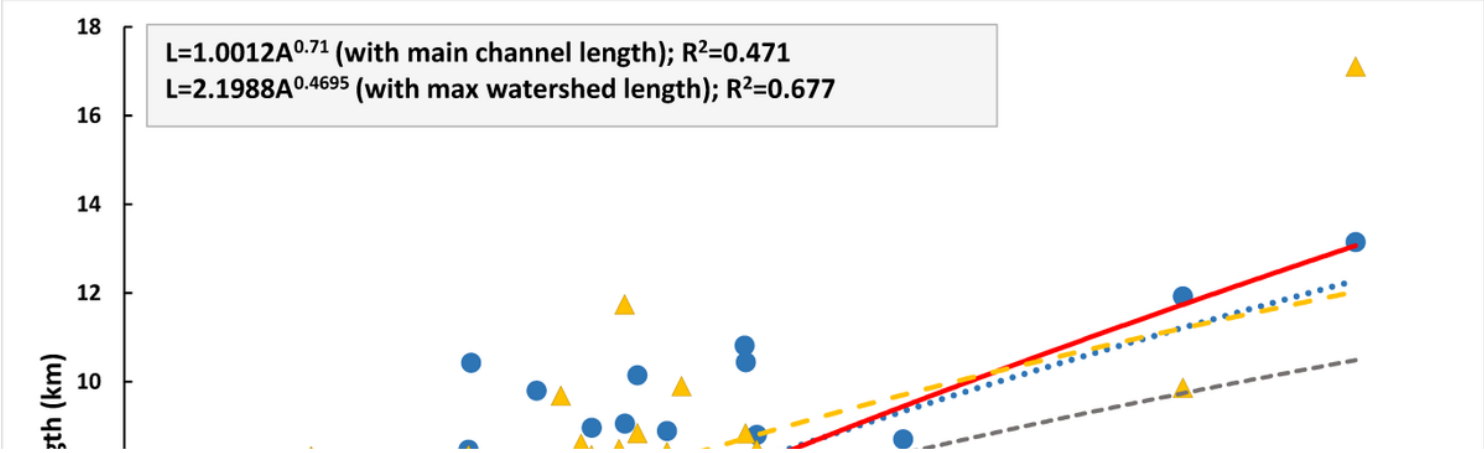

Figure 3

Length – area relationship on the measured watersheds. Cl: main channel length, L: maximum basin length, 1: trendline of the Hack's Law, 2: trendline of Montgomery's Law, 3: trendline of our calculation with main channel length, 4: trendline of our calculation with maximum basin length.

Figure 4

Relative relief map of the Mecsek microregion including our study area. A= boundary of study area, B= boundary of Mecsek microregion unit.

Figure 5

Stream orders in watersheds of Mecsek. A = border of the calculated watersheds, 1–5 = Strahler orders.

Figure 6

Highest Strahler-order (0–4) in every watershed. 1–53 = ID of watersheds.

Figure 7

Types of landuse in and around Mecsek. A: borders of the calculated watersheds, 1: continuous urban fabric, discontinuous urban fabric, industrial and commercial units, mineral extraction sites, sport and leisure facilities, 2: non-irrigated arable land, vineyards, fruit trees and berry plantations, complex cultivation patterns, land principally occupied by agriculture, with significant areas of natural vegetation, 3: broad-leaved forest, coniferous forest, mixed forest, 4: natural grasslands, transitional woodland-shrub, 5: inland marshes, water bodies.

Figure 8

Charts of correlations between some measured watershed parameters.

Figure 9

Flash flood hazard ranking map. Rank number (0 – 9), watershed ID (1 – 53).

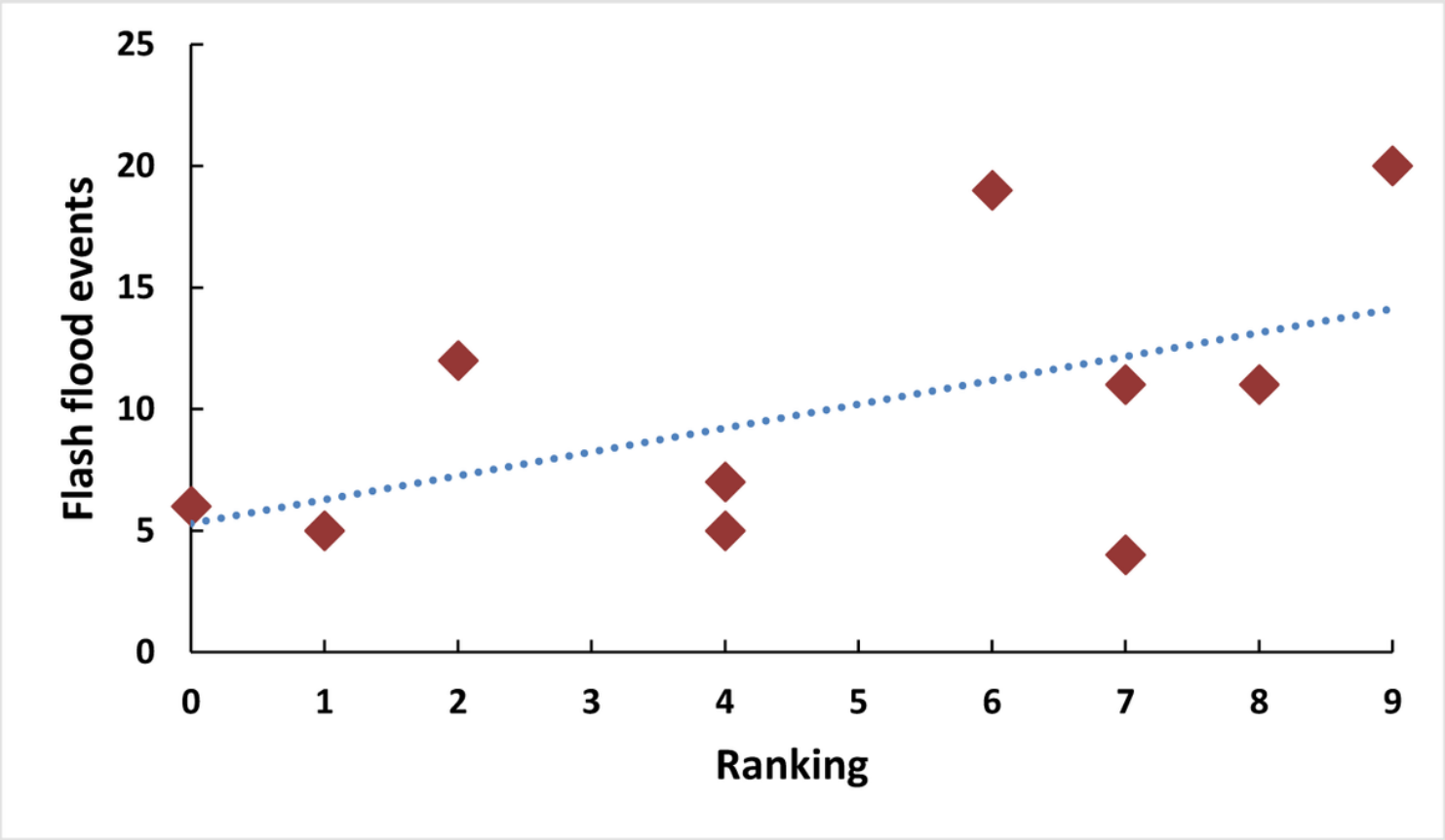

Figure 10

Chart of correlation between the number of flash flood events and the calculated flash flood hazard rank.